JOURNAL OF SOLID STATE CHEMISTRY 83, 255–266 (1989)

Transformations by Change in the Oxidation State Inside the V_2O_5–MoO_3 System Studied by Analytical TEM Technique

Z. C. KANG

Lab. de Microscopie Electronique Appliquée, Faculté des Sciences de St-Jérome, 13397 Marseille Cedex 13, France

Q. X. BAO

Beijing Research Institute of Chemical Industry, He Ping Li, Beijing, China

AND C. BOULESTEIX

Lab. de Microscopie Electronique Appliquée, Faculté des Sciences de St-Jérome, 13397 Marseille Cedex 13, France

Received February 13, 1989; in revised form June 28, 1989

An interesting reversible absorption process of oxygen atoms with changes over crystals from oxidizing to reducing conditions in the temperature range 450–650°C in the V_2O_5–MO_3 system has been investigated by analytical electron microscopy. The reversible transformation occurs from the V_2MoO_8 phase to the $(Mo_{0.3}V_{0.7})_2O_5$ phase. An "edge dislocation" plays the role of nucleus for the transition. A solid solution $(Mo_xV_{1-x})_2O_5$ ($x < 0.2$) must occur to balance the compositional variations.

1. Introduction

Recently, a very interesting reversible absorption of atomic oxygen that occurs with a change in the ambience over crystals from oxidation to reduction conditions in the temperature range 450–650°C has been discovered in the V_2O_5–MoO_3 system (*1*). To understand this phenomenon, X-ray diffraction patterns were obtained; these revealed the following: (a) During absorption of atomic oxygen the V_2O_5-type and V_2MoO_8 phases coexist; (b) under desorption of oxygen the $(Mo_{0.3}V_{0.7})_2O_5$ phase was formed. Therefore a reversible set of solid state reaction equations can be written as follows:

$$10\ (Mo_{0.3}V_{0.7})_2O_5 + 3\ O \rightarrow 6\ V_2MoO_8 + V_2O_5 \text{ (absorbing oxygen)} \quad (1)$$

$$6\ V_2MoO_8 + V_2O_5 - 3\ O \rightarrow 10\ (Mo_{0.3}V_{0.7})_2O_5 \text{ (releasing oxygen)}. \quad (2)$$

These equations clearly describe the observed reaction process, but it is difficult to understand the mechanism of the solid reaction. Several authors have already reported on this type of reaction in the V_2O_5–MoO_3 system (*2*, *3*) and discussed the structural model (*4*).

0022-4596/89 $3.00

For the characterization of this solid state reaction, the nature and structure of both phases, V_2MoO_8 and $(Mo_{0.3}V_{0.7})_2O_5$, must be understood.

Kihlborg and Eick reported structural data on these phases, obtained by X-ray diffraction (*5, 6*). The crystal structure of the $(Mo_{0.3}V_{0.7})_2O_5$ phase is characterized by the space group $C2$ (No. 5) with unit cell dimensions $a = 11.809$ (± 0.002) Å, $b = 3.652$ (± 0.001) Å; $c = 4.174$ (± 0.001) Å, and an angle $\beta = 90.56$ (± 0.02)°. The crystal structure of the V_2MoO_8 phase is characterized by the space group $C2$ (No. 5) with unit cell dimensions $a = 19.398$ (± 0.001) Å; $b' = \frac{1}{2}$, $b = 3.629$ (± 0.001) Å; $c = 4.117$ (± 0.001) Å; and an angle $\beta = 90.34$ (± 0.03)°.

The V_2MoO_8 phase consists of ReO_3-type slabs, infinitely long in two dimensions but only three octahedra in thickness (*5, 6*). These slabs are connected by edge sharing between component octahedra. The ideal arrangement is considerably distorted, mainly because of the displacement of the metal atoms from the centers of the octahedra. The vanadium and molybdenum atoms are distributed almost (but not quite) statistically over the two nonequivalent positions. The metal–oxygen bond lengths are generally intermediate between the corresponding values in the V_2O_5 and MoO_3 oxides. On the basis of the structure, a homogeneity range, $V_{2-x}Mo_{1+x}O_8$, where $x \geq 0$, is expected for this phase.

The structure of the $(Mo_{0.3}V_{0.7})_2O_5$ phase is of the same type as that of R–Nb_2O_5 and may be considered to be composed of MO_6 octahedra coupled in the same manner as in V_2O_5, although the distortion of the metal atoms within the octahedra follows a different pattern (*5, 6*). This distortion, as reflected in the considerable difference in the metal oxygen bond lengths, is intermediate in magnitude between that in V_2O_5 and that in MoO_3. Molybdenum and vanadium atoms are randomly distributed over the metal atom positions. It is obvious that the structure is closely related to that of the V_2MoO_8 phase.

Figure 1 displays the projections of both structures in the [001] orientation (*5, 6*). Figure 2 is the projection of both structures in the [010] direction. The distinct difference between the two structures is that in the V_2MoO_8 structure the slabs of ReO_3 type have a thickness of three octahedra rather than two as in the $(Mo_{0.3}V_{0.7})_2O_5$ structure, whereas the interconnection of the slabs remains the same. It is difficult to find a way to change one structure into another by crystallographic shear. However, when the structure of the V_2MoO_8 phase is transformed to that of $(Mo_{0.3}V_{0.7})_2O_5$, the corner-sharing slabs will be changed to edge-sharing types, with a concomitant release of oxygen atoms. In the reverse transformation from $(Mo_{0.3}V_{0.7})_2O_5$ to V_2MoO_8 oxygen atoms must be reabsorbed during the change from edge sharing to corner sharing of the octahedral slabs. The best method for observing this process is to use analytical electron microscopy with high spatial resolution so that this phenomenon may be followed at nearly the atomic scale.

2. Experimental Results

The samples were heated from 450 to 650°C in a thermobalance with flowing He or O_2. The sample was quenched when the sample weight gained or lost was a maximum. The compound was then dispersed by ultrasonic vibration and mounted on a holey carbon grid for electron microscopic observation. The electron microscope used was the JEOL 2000FX. The electron diffraction pattern, the composition, and the high-resolution image were obtained at virtually the same region.

2.1 Electron Diffraction and Composition Analysis of the Two Phases

The X-ray results demonstrated the existence only of the V_2O_5, the V_2MoO_8, and

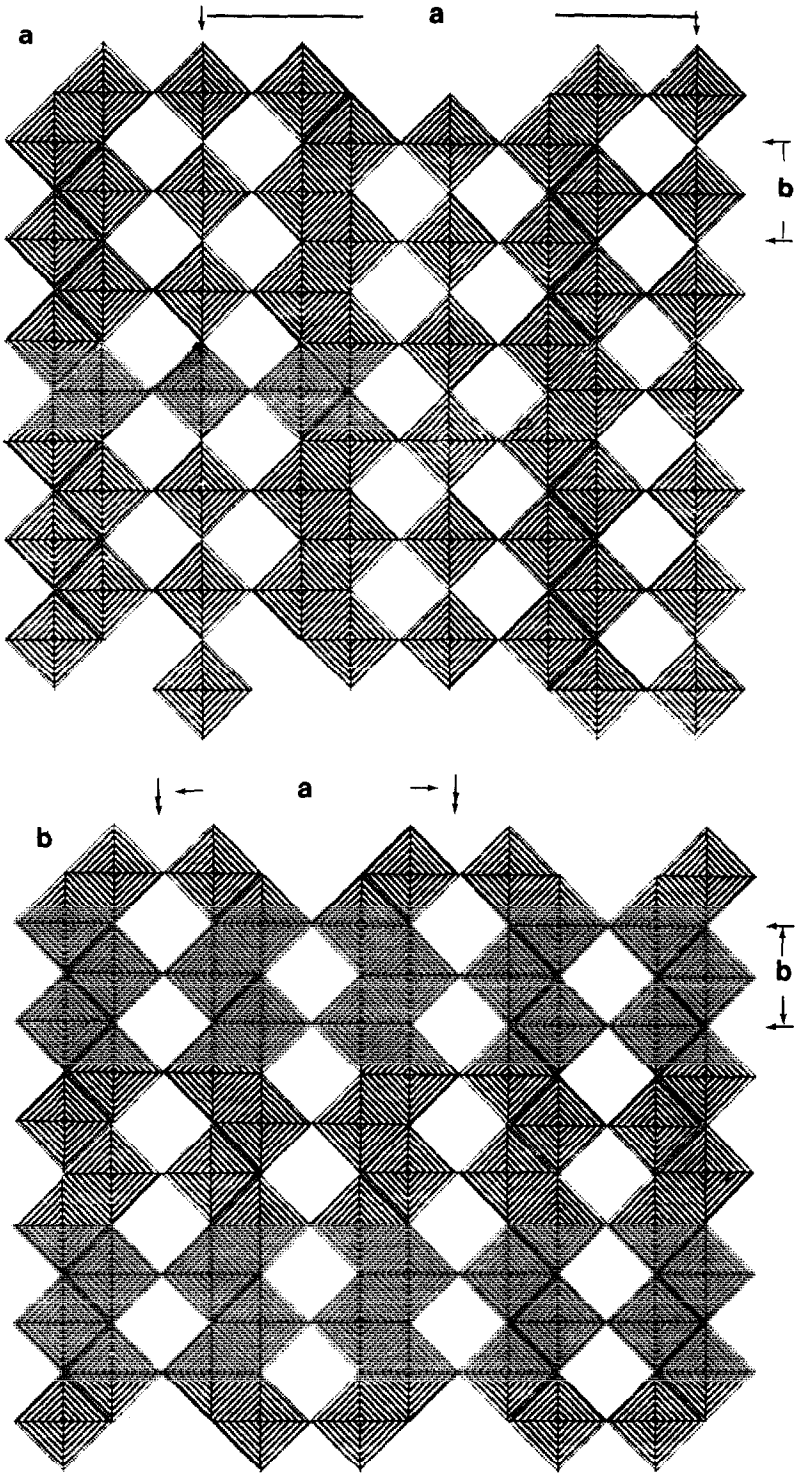

FIG. 1. (a) Projection of the V_2MoO_8 structure along the [001] direction. (b) Projection of the $(Mo_{0.3}V_{0.7})_2O_5$ structure along the [001] direction.

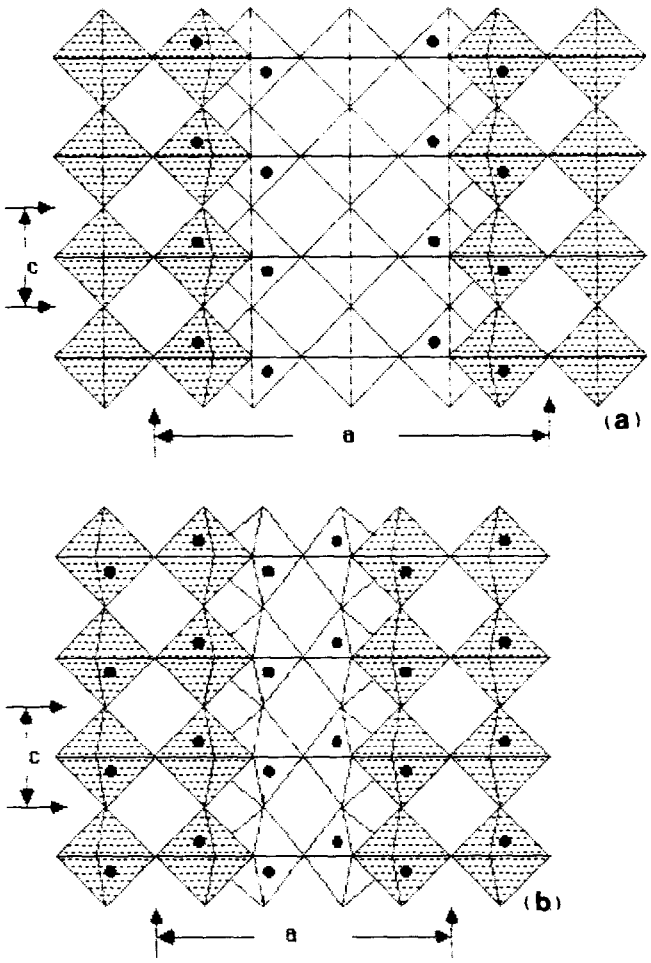

FIG. 2. (a) Projection of the V_2MoO_8 structure along the [010] direction. (b) Projection of the $(Mo_{0.3}V_{0.7})_2O_5$ structure along the [010] direction.

the $(Mo_{0.3}V_{0.7})_2O_5$ phases; it was therefore necessary to clarify the relations between the composition and diffraction data. Accordingly, we obtained composition and diffraction data from small crystals. We did not observe the V_2O_5 phase, which probably does not exist, but did find the $(Mo_y V_{1-y})_2O_5$ phase (y from 0.04 to 0.19). Figure 3 shows the typical X-ray energy dispersion (EDX) spectrum and the electron diffraction pattern of this phase. The diffraction pattern of this phase is the same as that for V_2O_5 but the composition is different; very likely a solid solution of molybdenum in a V_2O_5 oxide has been formed. We will now focus on the solid state reactions.

Figure 4 shows the electron diffraction patterns and X-ray energy dispersion spectra of V_2MoO_8 (Fig. 4a), and of $(Mo_{0.3}V_{0.7})_2O_5$ (Fig. 4b). The EDX data provide the atomic ratio of the two phases. The ratio C_V/C_{Mo} was ≥ 2 for the V_2MoO_8 phase, but $C_V/C_{Mo} \leq 2$ for the $(Mo_{0.3}V_{0.7})_2O_5$ phase. Electron diffraction patterns in the [001] zone are shown in Fig. 4a for the V_2MoO_8 phase, and in Fig. 4b for the $(Mo_{0.3}V_{0.7})_2O_5$

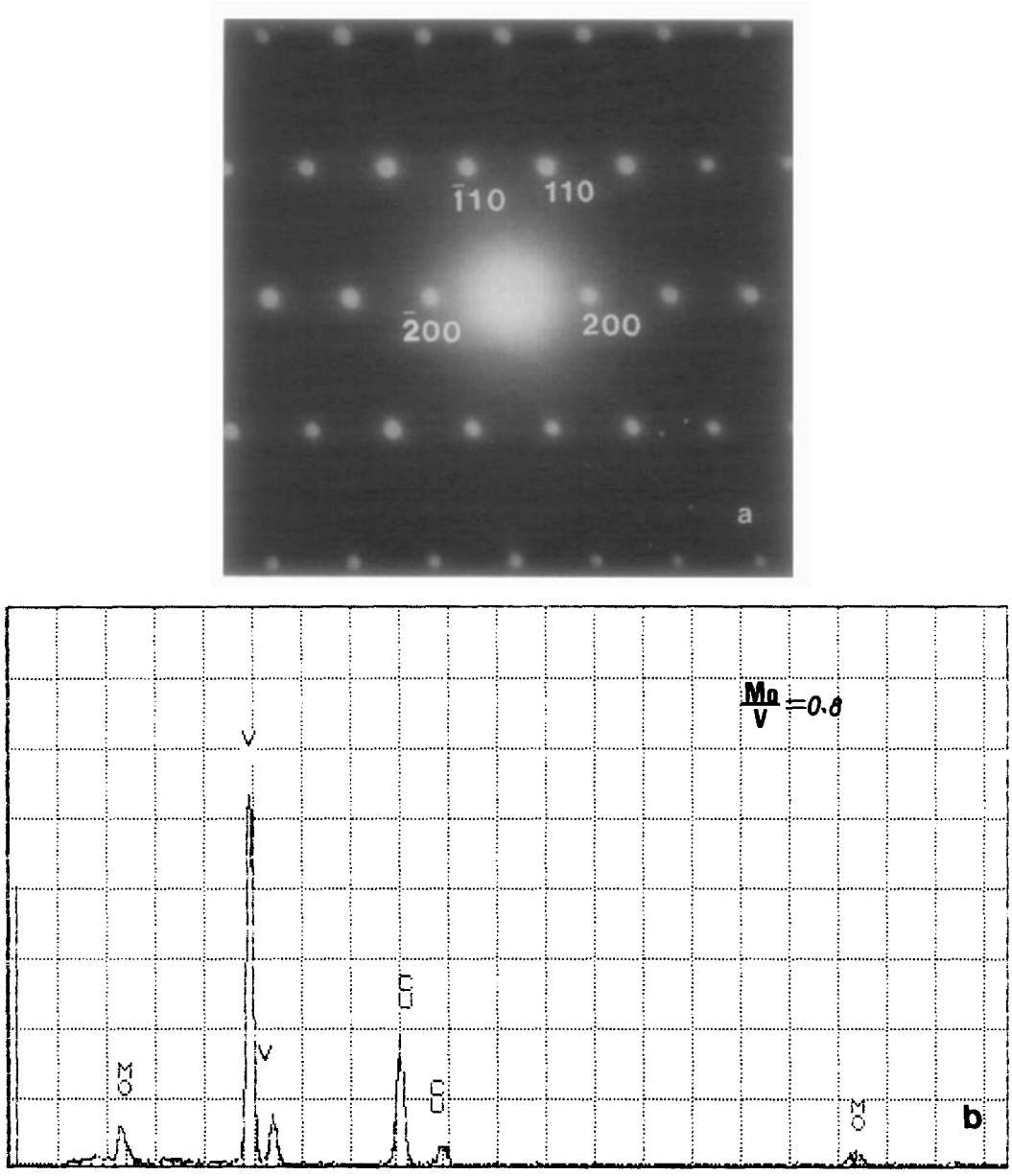

FIG. 3. (a) An electron diffraction pattern of the $(Mo_yV_{1-y})_2O_5$ phase. (b) Typical X-ray energy dispersion (EDX) spectrum of the $(Mo_yV_{1-y})_2O_5$ phase. The measured ratio of Mo and V atoms (Mo/V) is 0.8.

phase. Figure 4a displays a square array of stronger spots, separated by four weaker spots. The stronger spots correspond to the octahedral groups in the structure and the four extra spots correspond to their special arrangement in the V_2MoO_8 phase. Figure 4b, the $(Mo_{0.3}V_{0.7})_2O_5$ phase, shows the same array of strong spots but separated by two weaker spots. This is in agreement with the known structure (see Fig. 1).

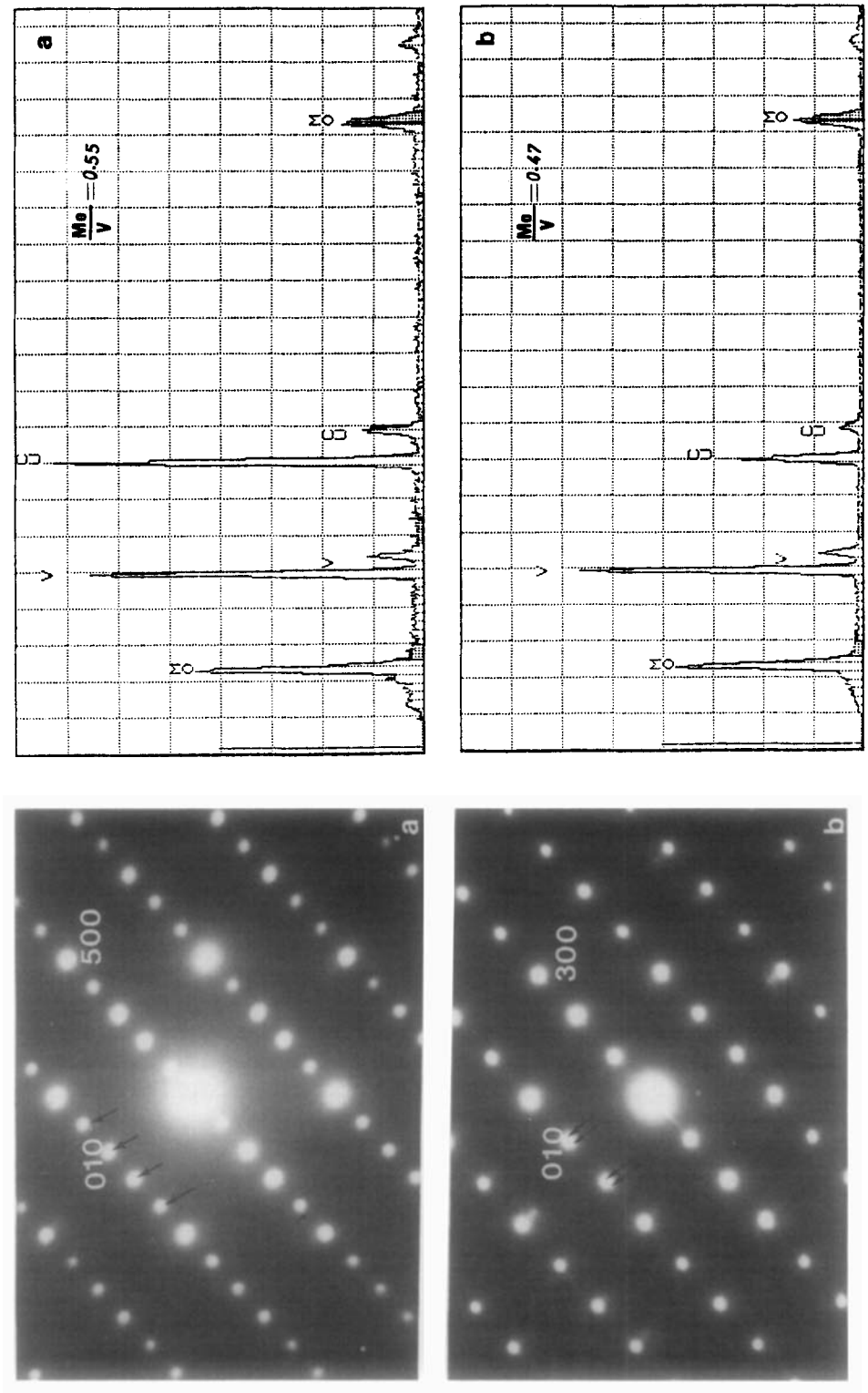

FIG. 4. (a) An electron diffraction pattern and EDX spectrum of the V_2MoO_8 phase. The measured ratio of Mo and V atoms (Mo/V) is 0.55. (b) An electron diffraction pattern and EDX spectrum of the $(Mo_{0.3}V_{0.7})_2O_5$ phase. The measured ratio of Mo and V atoms (Mo/V) is 0.47.

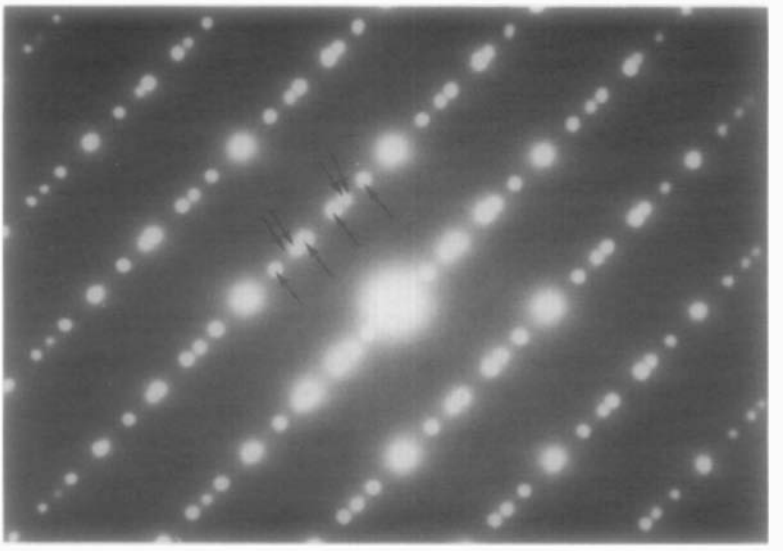

FIG. 5. An electron diffraction pattern of the coexisting V_2MoO_8 and $(Mo_{0.3}V_{0.7})_2O_5$ phases.

In some of the reduced samples the electron diffraction pattern shows both phases present, i.e., two and four extra spots between the square array of stronger spots (Fig. 5); under such conditions both phases coexist in the same region. The relationship between them can be seen in the high-resolution image.

2.2 Relationship between the Two Phases when Releasing Oxygen Atoms

Figure 6 exhibits the high-resolution images of V_2MoO_8 (a), of $(Mo_{0.3}V_{0.7})_2O_5$ (b), and of their intergrowth (c). The corresponding optical diffraction patterns obtained from these images have been inserted in each image. In the standard image the white dots can be understood as arising from tunnels between the octahedra columns. But the microscope cannot resolve tunnels separated by less than 3 Å, which occur in V_2MoO_8. Therefore, we observe larger intervals in the V_2MoO_8 image than in the $(Mo_{0.3}V_{0.7})_2O_5$ image.

The intergrowth part of the two phases is the most interesting region because it provides a clue for understanding how the solid state reaction occurs. This occurs in the region marked A in Fig. 6c. In this region the zigzag termination of a residual unreactive V_2MoO_8 phase inside the $(Mo_{0.3}V_{0.7})_2O_5$ phase exhibits the relationship between the two structures. Optical diffraction patterns taken from these areas and showing the different structures have been inserted. Terminations, marked by arrows in the figure, show that two fringes of the $(Mo_{0.3}V_{0.7})_2O_5$ phase start from one terminal fringe of the V_2MoO_8 phase. At the interface, on the right side of the two phases, one fringe of V_2MoO_8 phase has been partly split into two fringes of $(Mo_{0.3}V_{0.7})_2O_5$ phase. This can be understood by examining the relationships of the two structures, as Fig. 1 shows. In the structure of the V_2MoO_8 phase, one corner-sharing octahedral slab connects with two edge-sharing octahedral slabs, which are the only component slabs of the $(Mo_{0.3}V_{0.7})_2O_5$ phase. Thus, if this corner-sharing slab is lost in the transformation from V_2MoO_8 to $(Mo_{0.3}V_{0.7})_2O_5$, then both edge-sharing slabs will be con-

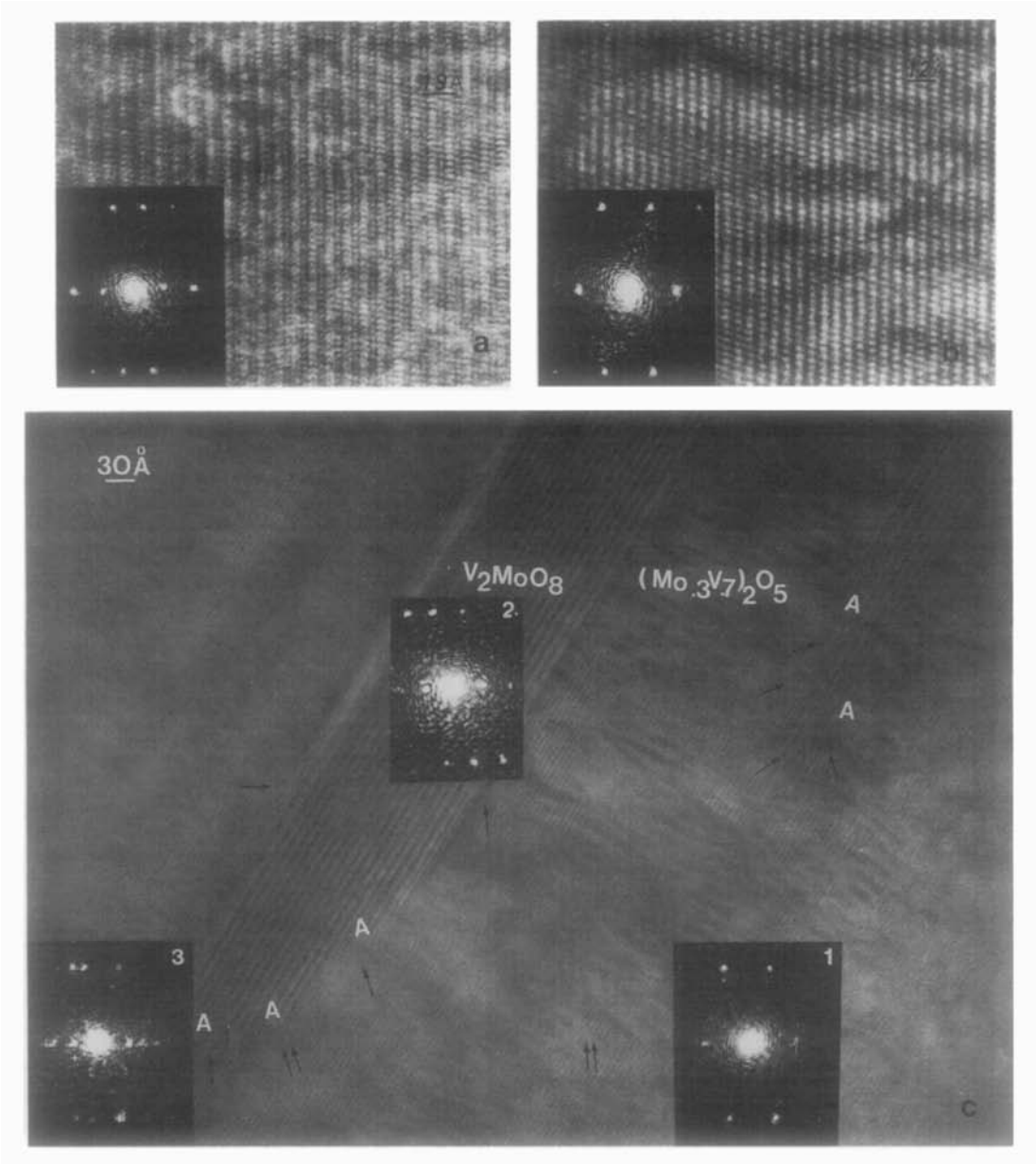

FIG. 6. High-resolution images taken along the [001] orientation: (a) the V_2MoO_8 phase; (b) the $(Mo_{0.3}V_{0.7})_2O_5$ phases; (c) the intergrowth of both phases, 1: optical diffraction of $(Mo_{0.3}V_{0.7})_2O_5$ phase, 2: optical diffraction of the V_2MoO_8 phase, 3: optical diffraction of the intergrowth region.

nected to each other to form the $(Mo_{0.3}V_{0.7})_2O_5$ phase. The volume is reduced in the transformation and the distance is reduced in the *a* direction, perpendicular to the fringes. Because *a* is smaller in $(Mo_{0.3}V_{0.7})_2O_5$ than that in V_2MoO_8, considerable distortion can be observed in this direction on the image (Fig. 6c), but no change of distances occurs along the plane perpendicular to the *a* direction. This can

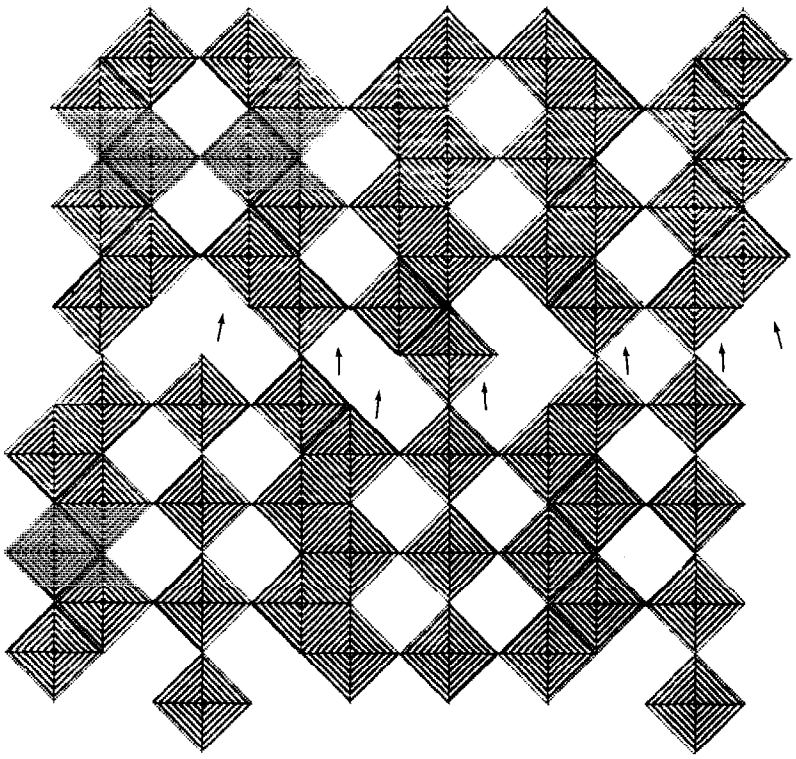

FIG. 7. A model for the interpretation of the transformation from the V_2MoO_8 phase to the $(Mo_{0.3}V_{0.7})_2O_5$ phase by the formation of double-edge shared octahedral slabs.

be expected to be a strainfree interface, and thus it can occur over large distances. This situation actually arises, as can be seen Fig. 6c. The model of the splitting process is given in Fig. 7. In the general case (one unit cell of the V_2MoO_8 structure), one double-edge-sharing octahedral slab is split and joined to the two corner-shared slabs to form two new double-edge-sharing slabs. During this process the number of corner- and edge-sharing events, for the double-edge-sharing slabs, does not change (see Fig. 7), but one more double-edge-sharing octahedral slab has been formed for each unit cell of the V_2MoO_8 phase. Two double-edge-sharing octahedral slabs have the same probability of splitting, giving rise to one defect, which is an "edge dislocation" in the $(Mo_{0.3}V_{0.7})_2O_5$ phase (marked by double arrows in Fig. 6). The new structure appears, as shown in Fig. 6, in the form of thin slices inside each other. This form reduces the strain energy and makes the transformation possible. No lattice strain is visible in the optical diffraction pattern taken at the interface; this indicates that no long-range distortion occurs, which is reasonable because the "dislocations" are located on the interface.

2.3 Defect as a Starting Point of the Phase Transition during Oxygen Absorption

Figure 8 shows a plane defect in the oxygen-releasing sample. It consists of edge dislocations of the $(Mo_{0.3}V_{0.7})_2O_5$ phase; considerable distortion occurs along the planar defect. We will now consider the ox-

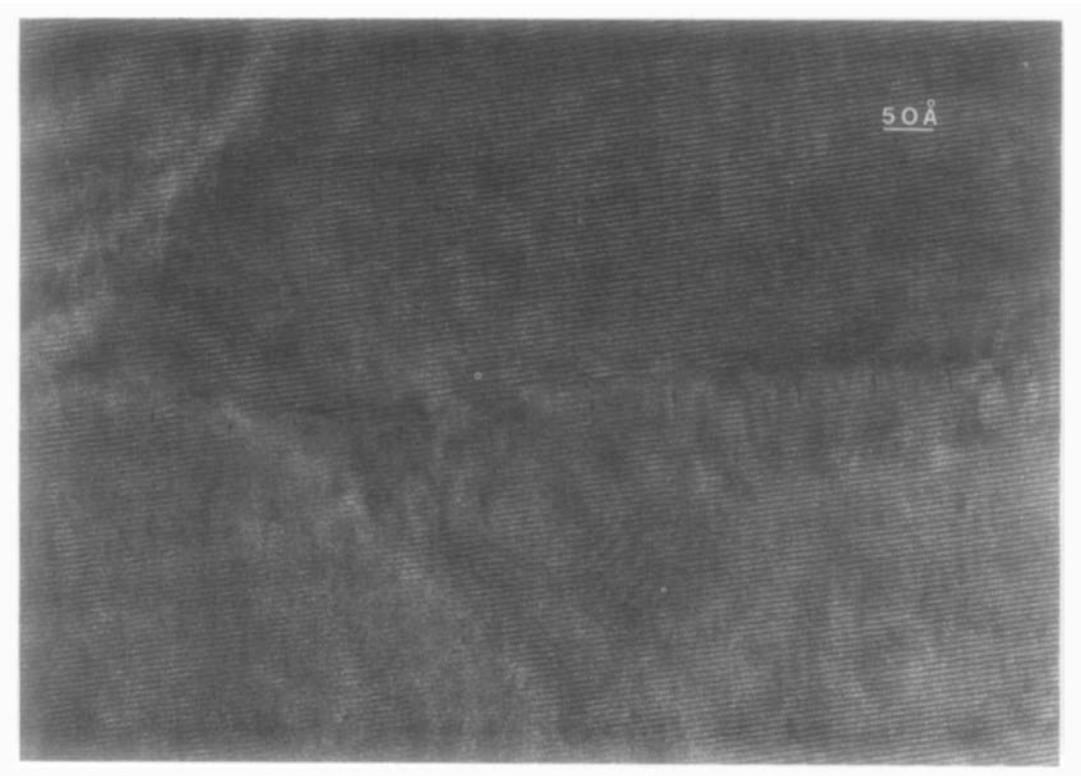

FIG. 8. A high-resolution image of a planar defect that generates the edge dislocations in the oxygen-releasing sample.

ygen absorption process for this phase. When an edge dislocation occurs in the $(Mo_{0.3}V_{0.7})_2O_5$ phase, the core of the dislocation plays the role of a nucleus of the V_2MoO_8 phase (Fig. 9). If the oxygen pressure is sufficient to drive the V_2MoO_8 phase growth, then a double-edge-sharing octahedral slab in the $(Mo_{0.3}V_{0.7})_2O_5$ phase is split and the V_2MoO_8 phase is formed. During this process, oxygen atoms should diffuse into the crystal. It is very interesting to note that in Fig. 6c considerable wavy contrast exists in the $(Mo_{0.3}V_{0.7})_2O_5$ phase, especially in the region between the two residual V_2MoO_8 phases. This wavy contrast also appears close to the planar defect in Fig. 8; this contrast is not a Moiré pattern. We also observed it in the nonstoichiometric rare earth compound $Tb_{12}O_{22}$ (*7*), where it had been explained in terms of an oxygen atom density modulation. We believe that we encounter here the same phenomenon due to the oxygen atom rearrangement and that this provides evidence for oxygen diffusion.

3. Discussion

The mechanism of reversible absorption and desorption of atomic oxygen atoms has been clearly described. However, from the postulated solid state reaction V_2O_5 must appear or disappear during the reaction, as Eqs. (1) and (2) indicate. However, no pure V_2O_5 was detected by microanalysis; thus there is no evidence for a V_2O_5 oxide in the absorbing or desorbing samples. However, we did encounter a considerable amount of molybdenum solid solution in V_2O_5 oxide,

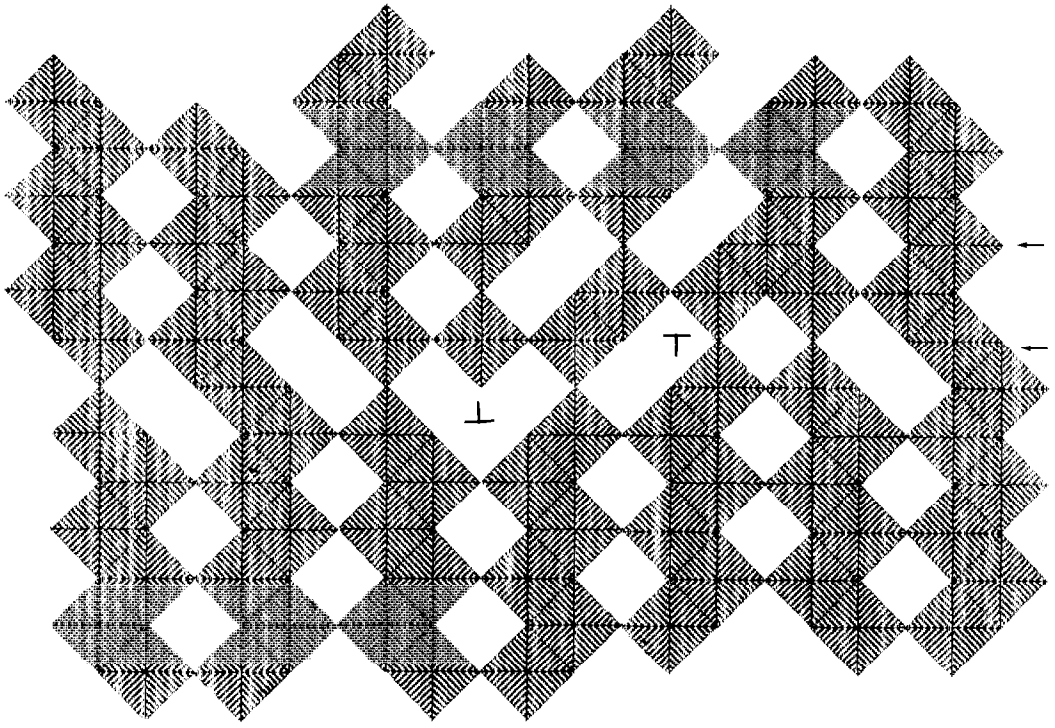

FIG. 9. A model of the edge dislocation in the $(Mo_{0.3}V_{0.7})_2O_5$ phase.

i.e., $(Mo_yV_{2-y})O_5$, where y ranges from 0.04 to 0.19. The diffraction patterns of the $(Mo_yV_{2-y})O_5$ oxide are the same as for the V_2O_5 oxide as shown in Fig. 3. In order to understand this feature, we used the electron beam to heat the absorbed oxygen sample in the microscope until the transformation occurred. Then, we analyzed the products by microanalysis and electron diffraction. The results shows that the reaction product has the same composition and structure as the $(Mo_yV_{2-y})O_5$ oxide; of course, the y value may be different for different pieces, but a pure V_2O_5 oxide was ever encountered. Thus, the solid state reaction is

$$(Mo_xV_{1-x})_2O_5 + O \rightarrow V_2MoO_8 + (Mo_yV_{2-y})O_5 \text{ (absorbing oxygen)} \quad (3)$$

$$V_2MoO_8 + (Mo_yV_{2-y})O_5 \rightarrow (Mo_xV_{2-x})O_5 + O \text{ (releasing oxygen)}, \quad (4)$$

where $y < x$ and $x \geq 0.2$. As Kihlborg pointed out, when $x \leq 0.2$, the structure of $(Mo_xV_{2-x})_2O_5$ is the same as that for V_2O_5, but if $x \geq 0.2$ the structure changes to that of the $(Mo_{0.3}V_{0.7})_2O_5$ phase. Therefore, the $(Mo_{0.3}V_{0.7})_2O_5$ phase should be transformed to the V_2MoO_8 phase, with formation of the $(Mo_yV_{2-y})O_5$ phase but not of V_2O_5. The y value can be variable.

It would be very interesting to try to make an *in situ* observation in the electron microscope and to observe the dynamic process of the reaction at the atomic scale.

The difference between the V_2O_5-type and the $(Mo_{0.3}V_{0.7})_2O_5$-type structures becomes significant when the distortions of the metal atoms from the centers of the oc-

tahedra are taken into account. Displacements occur predominantly along the direction of the c axis. As Fig. 2 shows, in V_2O_5 all metal atoms within an ReO_3-type slab are displaced in the same direction while in $(Mo_{0.3}V_{0.7})_2O_5$ they are shifted pairwise in opposite directions. Kihlborg pointed out that this was energetically more favorable from a purely electronic point of view. However, for the V_2MoO_8 phase the off-center displacements of the metal atoms form an intermediate between the V_2O_5 and the $(Mo_{0.3}V_{0.7})_2O_5$ phases since the displacement within the central octahedra of each slab goes in both directions. It alternates between $+z$ and $-z$ when going in the direction of the b axis, which is thereby doubled. Both types of relative displacements within neighboring octahedra are thus present simultaneously in the V_2MoO_8 structure. These situations are energetically very similar; thus when the atmosphere around the crystal is changed from oxidation to reduction, the structure can transform from one to the other.

4. Conclusion

According to composition microanalysis, electron diffraction, and high-resolution electron microscopy, we can provide the following mechanism of the reversible oxygen absorption and desorption phenomenon:

(1) During reduction, double-edge-sharing octahedral slabs in the V_2MoO_8 phase are split into two single octahedral slabs. They then connect with nearby corner-sharing octahedral slabs to form a new double-edge-sharing octahedral slab. By this means the structure of the $(Mo_{0.3}V_{0.7})_2O_5$ phase is formed.

(2) During the reaction a molybdenum solid solution of V_2O_5 oxide has been formed whose composition is variable.

(3) The defect described as an edge dislocation can be the nucleus or the reversible reconstruction reaction.

Acknowledgments

The authors are grateful to the CRMC2 for the use of the JEOL 2000FX electron microscope and to Mr. S. Nitshe for his assistance.

References

1. Q. X. Bao, to be published.
2. M. Najbar and S. Nizioi, *J. Solid State Chem.* **26,** 339 (1978).
3. J. G. Eon, E. Bordes, and P. Courtine, *C.R. Acad. Sci.* **C** 288, 485 (1979).
4. M. Najbar, *J. Chem. Soc. Faraday Trans. 1* **82,** 1673 (1986).
5. H. A. Eick and L. Kihlborg, *Acta Chem. Scand.* **20** 1658 (1966).
6. L. Kihlborg, *Acta Chem. Scand.* **21,** 2495 (1967).
7. Z. C. Kang, C. Boulesteix, and L. Eyring, *J. Solid State Chem.* **81,** 96 (1989).